Acta Pharmaceutica Sinica B 2021;11(11):3481−3492

Chinese Pharmaceutical Association
Institute of Materia Medica, Chinese Academy of Medical Sciences

Acta Pharmaceutica Sinica B

www.elsevier.com/locate/apsb
www.sciencedirect.com

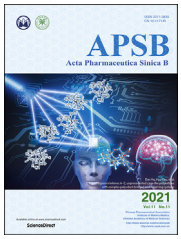

ORIGINAL ARTICLE

Bruceine D inhibits HIF-1α-mediated glucose metabolism in hepatocellular carcinoma by blocking ICAT/β-catenin interaction

Rui Huang[a,†], Lijun Zhang[a,†], Jinmei Jin[a,†], Yudong Zhou[a,c], Hongwei Zhang[a], Chao Lv[a], Dong Lu[a], Ye Wu[a], Hong Zhang[a], Sanhong Liu[a], Hongzhuan Chen[a,*], Xin Luan[a,*], Weidong Zhang[a,b,*]

[a]*Institute of Interdisciplinary Integrative Medicine Research, Shanghai University of Traditional Chinese Medicine, Shanghai 201203, China*
[b]*School of Pharmacy, Second Military Medical University, Shanghai 200433, China*
[c]*Department of Chemistry and Biochemistry, College of Liberal Arts, University of Mississippi, University, MS 38677-1848, USA*

Received 11 January 2021; received in revised form 21 April 2021; accepted 22 April 2021

KEY WORDS

Hepatocellular carcinoma;
Bruceine D;
HIF-1α;
Metabolism;
ICAT;
β-Catenin;
Tumor microenvironment;
Hypoxia

Abstract Hepatocellular carcinoma (HCC) is one of the leading causes of cancer-related deaths, characterized by highly hypoxic tumor microenvironment. Hypoxia-inducible factor-1α (HIF-1α) is a major regulator involved in cellular response to changes of oxygen levels, supporting the adaptation of tumor cells to hypoxia. Bruceine D (BD) is an isolated natural quassinoid with multiple anti-cancer effects. Here, we identified BD could significantly inhibit the HIF-1α expression and its subsequently mediated HCC cell metabolism. Using biophysical proteomics approaches, we identified inhibitor of β-catenin and T-cell factor (ICAT) as the functional target of BD. By targeting ICAT, BD disrupted the interaction of β-catenin and ICAT, and promoted β-catenin degradation, which in turn induced the decrease of HIF-1α expression. Furthermore, BD could inhibit HCC cells proliferation and tumor growth *in vivo*, and knockdown of ICAT substantially increased resistance to BD treatment *in vitro*. Our data highlight the potential of BD as a modulator of β-catenin/HIF-1α axis mediated HCC metabolism.

Abbreviations: BD, bruceine D; CETSA, cellular thermal shift assay; Cyt *c*, cytochrome *c*; DARTS, drug affinity responsive target stability; HCC, hepatocellular carcinoma; HIF-1α, hypoxia-inducible factor-1α; HIF-1β, hypoxia-inducible factor-1β; ICAT, inhibitor of β-catenin and T-cell factor; MST, microscale thermophoresis; ROS, reactive oxygen species.

*Corresponding authors.
E-mail addresses: hongzhuan_chen@hotmail.com (Hongzhuan Chen), luanxin@shutcm.edu.cn (Xin Luan), wdzhangy@hotmail.com (Weidong Zhang).
[†]These authors made equal contributions to this work.

Peer review under responsibility of Chinese Pharmaceutical Association and Institute of Materia Medica, Chinese Academy of Medical Sciences.

https://doi.org/10.1016/j.apsb.2021.05.009

1. Introduction

Hepatocellular carcinoma (HCC) is the leading cause of cancer incidence death, with a five-year survival rate less than 18%[1]. Although tremendous advances have been achieved in the development of new diagnostic techniques, chemotherapeutic agents, and therapeutic strategies, the successful treatment of HCC still remains a critical challenge due to drug resistance, distant metastasis, and limited survival rates[2,3].

In HCC tumor microenvironment, cancer cells are frequently exposed in a hypoxic state, and adapt to the relatively low oxygen levels through the hypoxia-inducible factor-1α (HIF-1α) signaling pathway[4]. HIF-1α exhibits a wide range of target genes[5], which functions to control a variety of signaling pathways, including cellular metabolism, angiogenesis, metastasis, and other properties of the HCC tumors[6]. Clinical data demonstrate that hypoxia and HIF-1α overexpression correlate closely with poor prognosis in HCC patients, indicating that HIF-1α might be a promising therapeutic target[7].

Bruceine D (BD) is one of the active compounds isolated from *Brucea javanica,* which has been widely used for the treatment of dysentery, inflammation, and warts with long tradition[8]. Mounting evidence links *B. javanica* with anti-tumor effects, and the petroleum ether extract of *B. javanica* has been approved to treat gastrointestinal tumors, HCC, and lung cancer in China[9–11]. BD, a quassinoid compound extracted from the seeds of *B. javanica* (Fig. 1A), has been proved to inhibit multiple cancer cells proliferation[8,12,13]. However, the mechanisms involved in BD-induced inhibition of HIF-1α have not yet been demonstrated, particularly its exact target.

Recently, several studies have focused on the interaction between WNT/β-catenin signaling and hypoxia in tumors. Coexistence of β-catenin and HIF-1α has been found both in human HCC cell lines and primary tumors, correlated with tumor aggressiveness and poor prognosis, and their expression levels were significantly positively related ($P = 0.034$)[14]. In our previous report, BD could inhibit HCC growth by targeting β-catenin/jagged1 pathways[15]. In present study, we demonstrated that BD could significantly inhibit the expression of HIF-1α and HIF-1α mediated HCC cell metabolism under hypoxic conditions. In addition, BD could inhibit HCC cells proliferation and tumor growth *in vivo*. Using biophysical proteomics approaches, we

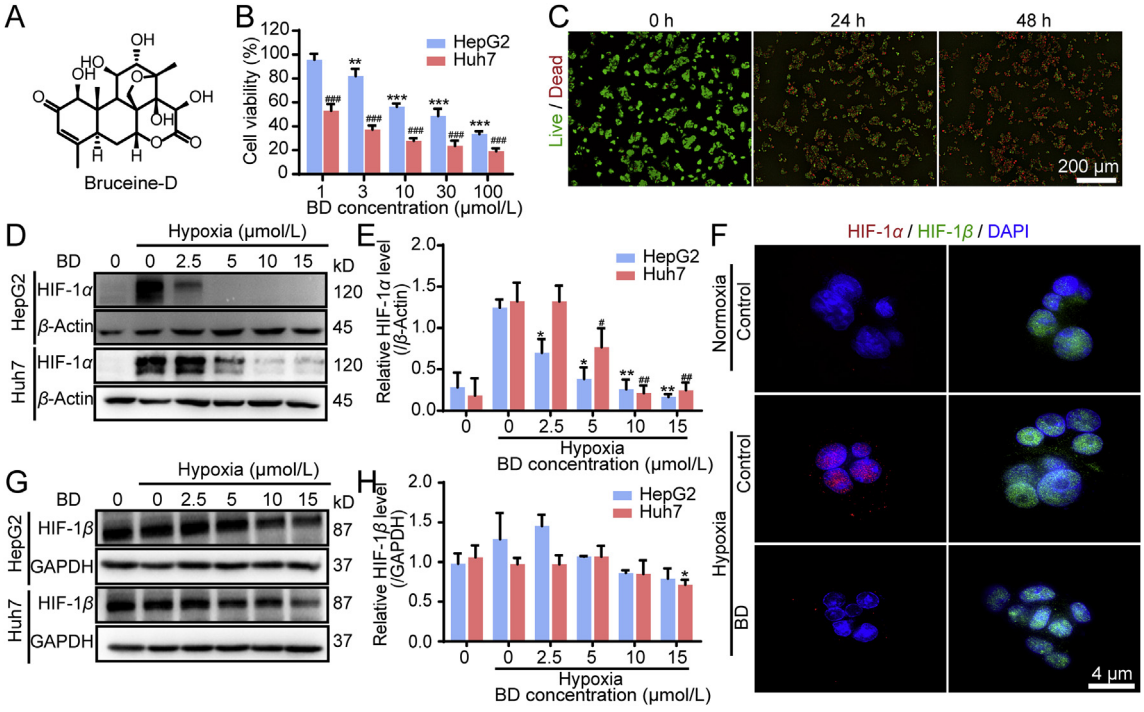

Figure 1 BD inhibited HCC cells proliferation and HIF-1α expression under hypoxia *in vitro*. (A) Chemical structure of BD. (B) HCC cells proliferation was examined using CCK-8 assay after treatment with BD for 48 h. (C) HepG2 cells after treatment with BD were stained with LIVE/DEAD cell viability/cytotoxicity kit (scale bar = 200 μm). (D) Western blot assay indicated that the expression of HIF-1α in hypoxic HepG2 and Huh7 cells showed significant decrease after treatment with BD for 12 h. (E) Statistical assay of the HIF-1α contents. Immunofluorescence assay for HIF-1α and HIF-1β in HepG2 cells treated with BD (F). The representative photographs of the cells are shown (scale bar = 4 μm). (G) Western blot assay indicated that the expression of HIF-1β in hypoxic HepG2 and Huh7 cells showed no change after treatment with BD for 12 h. (H) Statistical assay of the HIF-1β contents. Data are shown as mean ± SD ($n = 3$); * and $^{\#}P < 0.05$, ** and $^{\#\#}P < 0.01$, *** and $^{\#\#\#}P < 0.001$ *versus* the hypoxia alone group.

identified inhibitor of β-catenin and T-cell factor (ICAT) as the functional target of BD. By targeting ICAT, BD disrupted the interaction of β-catenin and ICAT, and promoted β-catenin degradation, which in turn induced the decrease of HIF-1α expression. Similarly, several other studies have also demonstrated that HIF-1α can be activated and enhanced by β-catenin. Our data highlight the potential of BD as a modulator of β-catenin/HIF-1α axis mediated HCC metabolism.

2. Materials and methods

2.1. Compounds and reagents

Bruceine D was isolated from the fruits of *Brucea javanica* (Linn.) *Merr* in our laboratory[16]. For *in vitro* experiment, BD was dissolved in 100% DMSO (Sigma, 01934-1L) at a final stock concentration of 50 mmol/L and stored at −20 °C as single used aliquot. The antibodies for GAPDH (5174s, 1:1000), β-actin (3700s, 1:1000), HIF-1α (36169s, 1:1000), β-catenin (8480s, 1:1000), PKM2 (4053T, 1:1000), HK2 (2867T, 1:1000), LDHA (3582T, 1:1000), Cyt *c* (11940T, 1:1000), HRP-conjugated anti-rabbit IgG (1:5000), HRP-conjugated anti-mouse IgG (1:5000), and Alexa Fluor 647 conjugated-anti-rat IgG (4418s, 1:1000) were purchased from Cell signaling technology (CST, Danvers, MA, USA). Primary antibodies for GLUT1 (ab115730, 1:1000), GLUT3 (ab191071,1:1000), HIF-1β (ab239366, 1:1000), ICAT (ab129011, 1:1000), HIF-1α (ab51608, 1:1000), and recombinant ICAT (ab101468) were both obtained from Abcam (Cambridge, UK). MCT4 (sc-376140, 1:1000) mouse IgG (sc-2025, 1:50) was procured from Santa Cruz (OR, USA). Recombinant human ICAT protein (ab101468) was obtained from Abcam (Cambridge, UK). Cycloheximide (Sigma, 5087390001) and MG132 (Sigma, SML1135) was obtained from Sigma (Shanghai, China).

2.2. Cell culture

HepG2 and Huh7 cells, originally obtained from Cell Bank of Shanghai institute of Cell biology, Chinese Academy of Sciences (SIBS, CAS), were cultured in DMEM (Gibco, 2120620) and 1640 (Gibco, 2192717) medium, respectively. HEK 293T, originally obtained from ATCC, was maintained in DMEM (Gibco, 2120620) medium. Both mediums were supplemented with 10% fetal bovine serum (Gibco, 10091148) and 1% penicillin−streptomycin (HyClone, SV30010). All cell lines used in the study were cultured in a humidified incubator (Thermo Fisher, USA) containing 5% CO_2 at 37 °C. Hypoxic conditions were performed with a hypoxia incubator chamber (Thermo Fisher, USA) flushed with gas mixture containing 1% O_2, 5% CO_2 and 94% N_2.

2.3. Cell viability assay

Cells were seeded in 96-well plates (5000 cells per well) and grown overnight. After treating with different concentrations of BD under hypoxic conditions for 48 h, the cells were incubated with CCK-8 solution (Dojindo, Japan) 10 μL per well for another 2 h. Absorbance at the wavelength of 450 nm was detected for further IC_{50} analysis. In addition, LIVE/DEAD cell viability/cytotoxicity kit (Beyotime, C2015S) was used to evaluate cell viabilities according to the manufacturer's instructions. In brief, after the treatment with BD under hypoxic conditions for 24 or 48 h, the cells were incubated with Calcein AM/PI mixture solution. The fluorescent images were captured on Cytation 5 (Biotek, USA; Calcein-AM, Ex/Em = 494/517 nm; PI, Ex/Em = 535/617 nm).

2.4. ROS measurement

HepG2 and Huh7 cells were cultured in 12-well plates at a density of 2×10^4 cells per well overnight. After being incubated with BD (10 μmol/L) for 24 h under hypoxic conditions, the cells were gently washed with PBS and followed by the incubation with 20 μmol/L 2′,7′-dichlorodihydrofluorescein (DCFH; Beyotime, S0033S) for 30 min. The images were captured with High Content Analysis System (PerkinElmer, USA) and the fluorescence signals were also detected by a flow cytometer.

2.5. Mitochondrial membrane potential (MMP) measurement

MMP of HCC cells were measured by using fluorescent probe JC-1 (Beyotime, C2006) and tetramethylrosamine (TMRM, MenChemExpress, HY-D0984A). The cell processing method was consistent with the ROS detection mentioned above. After treatment, the cells were gently stained with JC-1 and TMRM for 20 min at 37 °C, respectively. Also, the fluorescent intensity of JC-1 monomers (Ex/Em = 488/525 nm) and aggregates (Ex/Em = 525/590 nm) were observed on Cytation 5. The fluorescence signals of JC-1 (monomers and aggregates) and TMRM (Ex/Em = 530/592 nm) were detected by a flow cytometer.

2.6. Glucose uptake ability detection

Glucose uptake ability of HCC cells was measured by using the Glucose Assay Kit (Cayman, 11046) as described by manufacturer. In brief, the cells seeded in 96-well plates (2×10^4 cells per well) were cultured in DMEM medium (Gibco, 212059) without glucose or carbon sources and allowed to adhere to plate overnight. After being treated with BD under hypoxic conditions, the cells were incubated with 100 μmol/L 2-NBDG at 37 °C for 30 min. The fluorescent intensity was detected by Cytation 5.

2.7. L-Lactate content measurement

Intracellular and extracellular lactate contents of HCC cells were evaluated by using the L-Lactate Assay Kit (Cayman, 0521418). The cells were cultured in DMEM basic medium supplement with 10% FBS for 24 h. After the treatment with BD under hypoxia, the cell pellet and culture medium were harvested respectively for the measurement of lactate content by fluorometric assay.

2.8. Cell metabolism assay

The Mito Stress Test Kit (Agilent, 103015-100), Glycolytic Rate Assay Kit (Agilent, 103344-100), and ATP Rate Assay Kit (Agilent, 103592-100) were used to evaluate the oxygen consumption rate (OCR), glycolytic proton efflux rate (GlycoPER), and ATP production rates through the Seahorse Bioscience XF96 extracellular flux analyzer (Agilent Technologies), respectively. Cells were seeded into the Seahorse XF 96-well culture plates (10,000 cells per well) and maintained in complete culture medium overnight. Then the cells were incubated with BD under hypoxia for 24 h, and the cell culture medium was replaced with bicarbonate-free low-buffered assay medium (supplement with

10 mmol/L glucose, 1 mmol/L pyruvate, 2 mmol/L glutamine, and 5 mmol/L HEPES) in a 37 °C CO_2-free incubator for 1 h. After base-line measurement, oligomycin, FCCP, and rotenone/antimycin A were added for the detection of OCR value. Similarly, rotenone/antimycin A and 2-DG (inhibitor of glycolysis) were added at the time points specified according to the manufacturer's protocols for the measurement of GlycoPER value. Also, the ATP production rate of mitochondrial oxidative phosphorylation and glycolysis was measured in the presence of oligomycin and rotenone/antimycin A.

2.9. Transient transfection

siRNA and NC oligonucleotide sequences were synthesized by GenePharma (Shanghai, China). The sequence of siICAT and siβ-catenin were list in Supporting Information Table S1. The plasmids coding wild type and mutant peGFP-ICAT were synthesized by GenScript Biotechnology Co., Ltd. (Nanjing, China). The sequences of the wide type and mutant peGFP-ICAT plasmid oligonucleotides were listed in supporting information (Supporting Information Table S2). Transfection was performed with TransMate (GenePharma) according to the manufacturer's protocols. Cells were harvested for assay 48 h after transfection.

2.10. Drug affinity responsive target stability (DARTS) assay

HepG2 and Huh7 cells were lysed in 500 μL NP-40 containing freshly added protease (Roche, 4693116001) and phosphatase inhibitors (Roche, 4906837001), respectively. The cell lysate was equally divided into two tubes and then incubated with BD (100 μmol/L) and an equal volume of DMSO for 1 h at room temperature, respectively. After incubation, the mixture was divided into 100 μL aliquot in tubes and digested with pronase (Roche, 10165921001) in various doses at room temperature for 30 min. Then the digestion was stopped by adding protease inhibitors, and the samples were used for mass spectrometry (Q Exactive HF-X, Thermo Fisher, USA) experiment and Western blot analysis.

2.11. Microscale thermophoresis (MST)

The MST measurement for the binding of BD to ICAT was performed using Monolith NT.115 (NanoTemper). In brief, the HEK 293T cell lysate was collected after 48 h transfection with the wide type or mutant pEGFP-ICAT plasmid. The level of ICAT/EGFP was verified by measuring the total fluorescence. For binding studies, the lysate was diluted 100-fold using standard buffer [50 mmol/L HEPES (pH 7.5), 50 mmol/L NaCl, 10 mmol/L $CaCl_2$, 5 mmol/L DTT, and 0.05% Tween-20] to provide the optimal level of the fluorescent protein in the binding reaction[17]. BD was titrated at a 1:1 diluted 16 times beginning at a concentration of 1 mol/L. Subsequently, 5 μL cell lysate was mixed with 5 μL BD in different concentrations. After 15 min incubation at room temperature, all the samples were loaded into MST NT.115 standard glass capillaries and measurement was carried out at 20% MST power and 75% excitation power using the MO. Control software.

2.12. Cellular thermal shift assay (CETSA)

This assay was performed as previously described[18]. Briefly, the lysate of HepG2 and Huh7 cells was equally divided into two tubes and then incubated with BD (100 μmol/L) and DMSO for 1 h at room temperature, respectively. After incubation, the mixture was divided into 100 μL aliquot in tubes and heated for 4 min at the indicated temperature. After cooling for 4 min at room temperature, the samples were boiled immediately after adding SDS-PAGE loading buffer and analyzed by Western blot.

2.13. Western blot analysis

HCC cells were treated with various concentrations of BD as mentioned previously, then, the cells were collected and lysed in ice-cold NP-40 buffer containing protease inhibitors. The total protein was quantified with BCA assay kit (Beyotime, P0010S). Then the proteins were separated in SDS-PAGE and transferred onto PVDF membranes (GE, 10600021). The PVDF membranes were blocked in Tris-buffered saline containing 1% Tween-20 (TBST, pH 7.4) with 5% non-fat milk and incubated with primary antibodies. After washing with TBST three times, the membranes were incubated with secondary antibodies. Detection was performed by gel Imaging System (Tanon, China), and the bands were analyzed by densitometry using Image J software (NIH, USA). GAPDH or β-actin was used as an internal control.

2.14. Quantitative real-time PCR analysis

Total RNA from the cells was extracted with Trizol (Invitrogen Carlsbad, CA, USA) according to the manufacturer's protocols. The SYBR Green-based qRT-PCR (Thermo Fisher) was performed to examine the relative *HIF-1α* mRNA level which was normalized with *GAPDH*. The sense and antisense primers for *HIF-1α* were 5′-CTCAAAGTCCGACAGCCTCA-3′ and 5′-CCCTGCAGTAGGTTTCTGCT-3′; for *GAPDH* were 5′-CACCCACTCCTCCACCTTTG-3′ and 5′-CCACCACCCTGTTGCTGTAG-3′.

2.15. Immunofluorescence analysis

HepG2 cells were plated on 35 mm glass plates and treated with 10 μmol/L BD for 24 h under hypoxic conditions. Then the cells were incubated with HIF-1α or HIF-1β (1:200) antibody after washing with PBS, and followed by incubating with the fluorescent-labeled secondary antibody. After DAPI staining, the fluorescence images were captured by using GE DeltaVision OMX SR (GE, USA). Cells without BD treatment were used as control.

2.16. Co-immunoprecipitation (Co-IP)

HepG2 cells were seeded in 10 cm culture dishes overnight and incubated with 10 μmol/L BD or equal amount of DMSO, and exposed to hypoxia for 3 h. After incubation, the cells were collected and lysed in 300 μL pre-cooled IP lysis buffer (Beyotime, P0013) containing freshly added protease and phosphatase inhibitors. The equal amounts of protein samples were adjusted to 500 μL and incubated with indicated antibodies overnight, and then incubated with a mixture of Protein A beads (Santa Cruz) for 4 h at 4 °C. The beads were collected and washed with pre-cooled IP lysis buffer three times. Finally, the samples were eluted in 2 × SDS loading buffer (Epizyme, LT103) for Western blot analysis.

2.17. Animal experiment

Five-week-old male BALB/c nude mice were obtained from Shanghai Slake Experimental Animal Co., Ltd. and housed under specific pathogen-free conditions. All the animal experiments were approved by Committee on the Ethic of Animal experiment of the Shanghai University of Traditional Chinese Medicine (SHUTCM), which complied with the national and international guidelines. For *in vivo* studies, 5×10^6 Huh7 cells in 100 μL serum-free culture medium were subcutaneously injected into the right flanks of mice. When the tumor volume reached 70−100 mm^3, the mice were randomly divided into 3 groups ($n = 5$ per group): control and BD (0.75, and 1.5 mg/kg). PBS or BD was administered daily *via* tail vein injection for 14 days. The tumor volume and body weight were monitored every two days. Tumor volume was calculated using Eq. (1):

$$\text{Volume } (mm^3) = \text{Length} \times (\text{Width}^2)/2 \quad (1)$$

After two weeks, the mice were sacrificed and tumors were stained for hematoxylin and eosin (H&E), TUNEL, Ki-67, HIF-1α, and β-catenin. Also, protein expression of HIF-1α, β-catenin, GLUT1/3, and LDHA was detected using Western blot.

2.18. Statistical analysis

Statistical analysis was conducted by using GraphPad Prism 7.0 software (La Jolla, CA, USA). Data were presented as means ± standard deviation (SD) from at least three-independent experiments. All experiment data were statistically evaluated by using two-tail student's *t*-test or one-way ANOVA with Tukey's multiple comparison tests. Values of $P < 0.05$ were considered significant.

3. Results

3.1. BD exhibited anti-cancer activity and inhibited cell proliferation in vitro

HCC constantly suffer from hypoxia because of faculty vascularization and intense metabolic activity[4]. To assess the cytotoxic effect of BD on HCC cells under hypoxic conditions, HepG2 and Huh7 cells were treated for 48 h with different concentrations of BD. CCK-8 assay exhibited that BD could dose-dependently inhibit HepG2 and Huh7 cell viability under hypoxic conditions. The IC_{50} values were 8.34 and 1.89 μmol/L, respectively (Fig. 1B). The anti-cancer effects of BD (10 μmol/L) were further confirmed by the Calcein-AM and PI dual staining assay. These results reveal strong time-dependent inhibition of HepG2 and Huh7 proliferation (Fig. 1C and Supporting Information Fig. S1).

Hypoxia in HCC cells trigger overexpression of HIF-1α, and clinical research has confirmed that overexpression of HIF-1α is associated with cancer progression and shorter survival in HCC patients[14]. To investigate the effects of BD on HIF-1α expression in HCC cells, we incubated HepG2 and Huh7 cells with BD and exposed the cells to hypoxia (1% O_2) for 12 h. As shown in Fig. 1D and E, HIF-1α expression was strongly suppressed by BD from 2.5 to 15 μmol/L in two cell lines, respectively. Similarly,

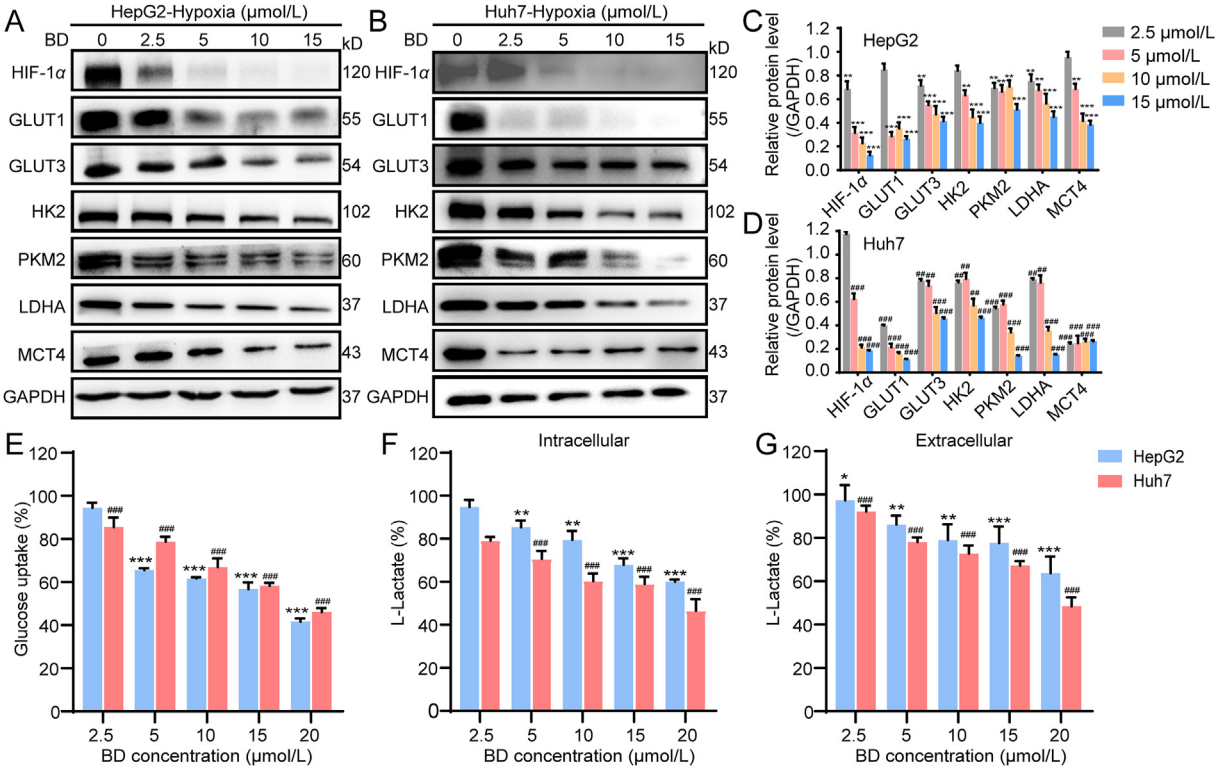

Figure 2 BD induced metabolic reprogramming in HCC cells under hypoxic conditions. BD treatment for 24 h reduced the protein expression of HIF-1α, GLUT1/3, HK2, PKM2, LDHA and MCT4 in HepG2 (A) and Huh7 (B) cells. Statistical assay of the relative protein contents in HepG2 (C) and Huh7 (D) cells. Treatment with BD for 24 h under hypoxia (1% O_2) decreased glucose uptake of HCC cells in a dose-dependent manner (E). Using L-Lactate Kit assay, BD treatment for 24 h decreased intracellular and extracellular lactate levels of HCC cells (F and G). Data are shown as mean ± SD ($n = 3$). * and $^{\#}P < 0.05$, ** and $^{\#\#}P < 0.01$, *** and $^{\#\#\#}P < 0.001$ *versus* the hypoxia alone group.

immunofluorescence revealed that the expression of the HIF-1α was significantly reduced in HepG2 cells with BD treatment at 10 μmol/L (Fig. 1F). In contrast to the significant decrease of HIF-1α levels after treatment with BD from 2.5 to 15 μmol/L, the expression of HIF-1β only declined at high concentration of BD (15 μmol/L) in Huh7 cells (Fig. 1F–H).

3.2. *BD inhibited glucose metabolism in HCC cells under hypoxic conditions*

Activation of HIF-1α pathway amplifies glycolysis by upregulating expression of many metabolism-related target genes such as GLUT1/3, PKM2, HK2, LDHA, MCT, thereby potentiating energy production to support tumor growth[19]. Here, BD was proved to suppress the expression of GLUT1/3, PKM2, HK2, LDHA, MCT4 in HepG2 and Huh7 cells from 2.5 to 15 μmol/L (Fig. 2A–D). To investigate whether BD regulated the aerobic glycolysis of HCC cells, we first used fluorescence labelled glucose 2-NBDG to measure glucose uptake in HCC cells. These results indicate that BD significantly decreased the glucose uptake in a dose-dependent manner (Fig. 2E). In addition, BD treatment decreased intercellular and extracellular L-lactate concentrations (Fig. 2F and G), indicating that BD could reduce L-lactate production and efflux of HCC cells under hypoxia.

Previous results demonstrated that BD could inhibit glucose uptake, L-lactate production, and L-lactate efflux in HCC cells. Therefore, we further explored whether BD had an inhibition effect on oxygen consumption rate (OCR), an indicator of mitochondrial respiration, as well as glycol-PER, which reflected glycolytic flux[20]. These results show that the OCR and glyco-PER were significantly reduced after BD treatment for 24 h (Fig. 3A–D, 3E–H), indicating that BD reduced the rate of glycolysis and mitochondrial respiration of both HCC cells. It was known that accumulation of ATP could be generated during aerobic glycolysis and mitochondrial respiration. Unsurprisingly, we found that ATP production was significantly decreased after BD treatment in a dose-dependent manner in HepG2 and Huh7 cells, respectively (Fig. 3I and J).

3.3. *BD treatment reduced ROS level and decreased MMP in HCC cells*

Mitochondria play a vital role in cellular metabolism[21]. The mitochondrial membrane potential (MMP) generated by proton pumps is an essential component for healthy mitochondrial function[22]. Dysfunctional mitochondria are characterized as MMP loss and reduced ATP generation. JC-1 fluorescence was first detected by microscopy and flow cytometry to determine the MMP in HCC cells. The results demonstrated that BD (10 μmol/L) significantly induced mitochondrial dysfunction as indicated by MMP loss (Fig. 4A, C, E, and F). Moreover, the decline of MMP was double-checked by application of TMRM dye, which obtained the similar conclusions (Fig. 4G). Given the inhibition effect of BD on mitochondrial oxidative phosphorylation, we next investigated whether BD affected mitochondrial ROS generation. Our results reveal that BD treatment inhibited ROS expression in both HCC cell lines at 10 μmol/L (Fig. 4B, D, and H). Cytochrome *c* (Cyt *c*) is a multifunctional protein, playing an important role in the mitochondrial electron transport chain, mitochondrial oxidative phosphorylation, and ROS balance[23]. As shown in Fig. 4I and J, BD decreased the

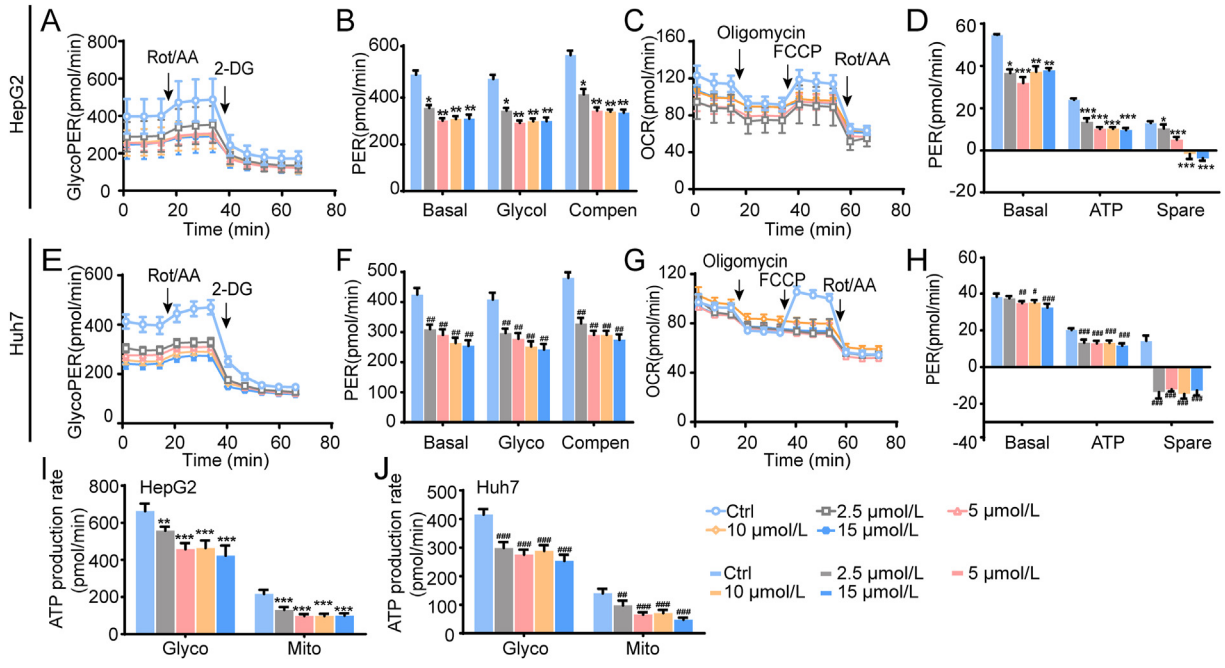

Figure 3 BD induced metabolic reprogramming in HCC cells under hypoxic conditions. (A, B, E, and F) Treatment with BD for 24 h under hypoxia (1% O_2) significantly decreased glycolytic capacity of HepG2 (A and E) and Huh7 (B and F) cells in a dose-dependent manner. Treatment with BD for 24 h under hypoxia (1% O_2) significantly inhibited OCR in HepG2 (C and D) and Huh7 (G and H) cells, respectively. Treatment with BD at different concentrations could decrease ATP production in HepG2 (I) and Huh7 (J) cells. All the experiments were performed by the Agilent's Seahorse Bioscience XF96 Extracellular Flux Analyzer. Data are shown as mean ± SD ($n = 3$). * and $^{\#}P < 0.05$, ** and $^{\#\#}P < 0.01$, *** and $^{\#\#\#}P < 0.001$ *versus* the hypoxia alone group.

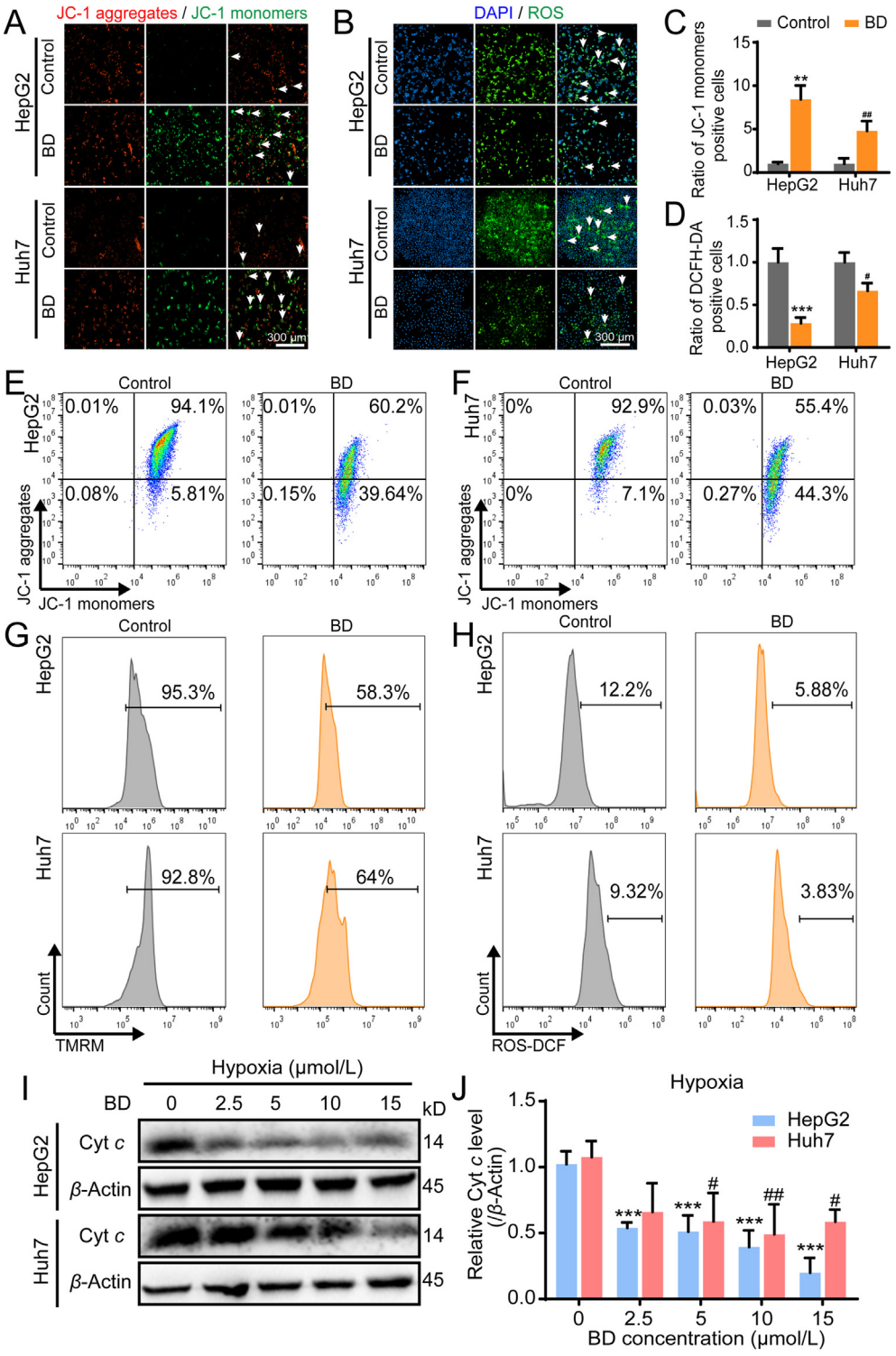

Figure 4 BD treatment induced MMP loss and decrease of ROS levels in HCC cells. Using JC-1 (A, C, E, and F) and TMRM (G) as detector, BD (10 μmol/L) treatment decreased MMP in HepG2 and Huh7 cells under hypoxia (1% O_2). (B, D, and H) DCFH-DA analysis showed that BD (10 μmol/L) treatment significantly decreased ROS levels in HepG2 and Huh7 cells. (I) BD reduced the protein expression of Cyt *c* in HepG2 and Huh7 cells. (J) Statistical assay of the relative protein contents in HepG2 and Huh7 cells. Data are shown as mean ± SD ($n = 3$). * and $^{\#}P < 0.05$, ** and $^{\#\#}P < 0.01$, *** and $^{\#\#\#}P < 0.001$ *versus* the hypoxia alone group.

protein level of Cyt *c* in a dose-dependent manner, indicating the injury of mitochondria.

3.4. *ICAT was a direct target of BD*

BD could inhibit HIF-1α and HIF-1α mediated glycolysis; however, the molecular target of BD in HCC cells still remained unclear. To investigate the molecular target of BD in HIF-1α regulation, we performed DARTS assay to identify the potential molecular target of BD with the principle that small-molecule binding proteins were protected and enriched during proteolysis. Using DARTS-based quantitative proteomics approach by mass spectrometry (MS), we identified a list of putative direct binding proteins (Supporting Information Table S3). In our previous study, BD was proved to inhibit β-catenin in HCC cells[15]. Considering the coexistence of β-catenin and HIF-1α and their significant positively related expression levels in HCC[14], the proteins which also connected with β-catenin signaling were prioritized for follow-up. According to the literature, ICAT was known as an inhibitor of β-catenin signaling[24]. Immunoblot analysis of DARTS sample further revealed the increased stabilization of ICAT during the proteolysis process when treated with BD at 100 μmol/L in HepG2 (Fig. 5B and D) and Huh7 (Fig. 5F and H) cells. Then, we performed CETSA which allowed the detection of physical binding of small molecules to target proteins, which proved that BD (100 μmol/L) could increase the thermal stability of ICAT in the intact living HepG2 (Fig. 5C and E) and Huh7 (Fig. 5G and I) cells at 49 °C and 52 °C.

The potential covalent or non-covalent binding of BD with ICAT was analyzed by mass spectrometry. The results show that the molecular weight of recombinant ICAT (11 kDa) had not changed after incubation with BD at various concentration (20 and 100 μmol/L), indicating that no covalent binding was formed between BD and ICAT (Supporting Information Fig. S2). And there is no cysteine (C) in the amino acids sequence of ICAT (Supporting Information Table S4), which may decrease the possibility of covalent binding. To further investigate the possible binding pattern between BD and ICAT domain, we performed a molecular docking analysis. The docking results prove that a hydrogen bond was generated between BD and Lys 28 on ICAT (Fig. 5A), and three hydrophobic interactions between BD and ICAT at Leu24, Leu52, and Met25 could also be found. To verify the DARTS, CETSA, and docking data, we determined the direct binding between BD and ICAT by MST assay. Expectedly, BD readily bound to ICAT with a K_d estimated at 33 μmol/L (Fig. 5J). To verify the important role of Lys28 in the complex interacting, we prepared a mutant ICAT by site-directed mutagenesis, further MST studies showed that the binding affinity of BD and mutant

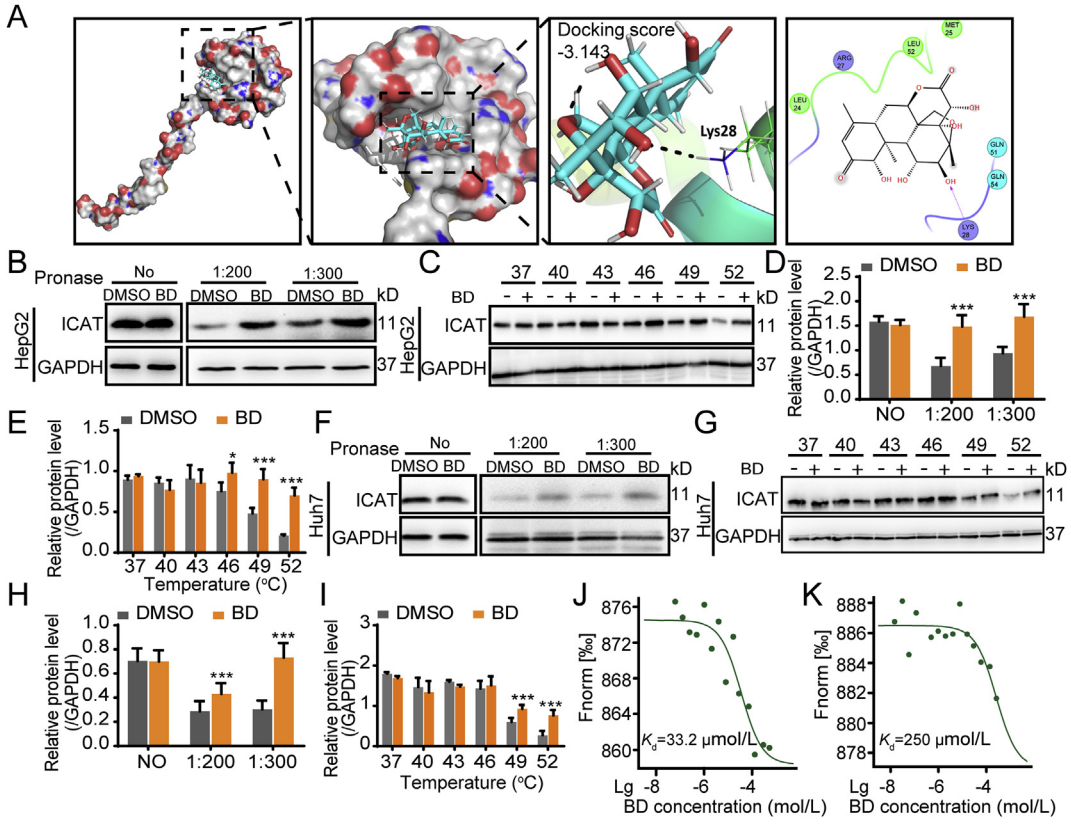

Figure 5 BD directly bound to ICAT. (A) Computer simulation of BD binding to ICAT, and a hydrogen bond was generated between BD and Lys 28 on ICAT. Immunoblot analysis of DARTS sample further revealed the increased stabilization of ICAT during the proteolysis process in HepG2 (B and D) and Huh7 cells (F and H). BD significantly increased the thermal stability of ICAT in CETSA assay at 49 °C and 52 °C in HepG2 (C and E) and Huh7 cells (G and I). (J) MST analysis of BD binding to wild type ICAT (K_d = 33.2 μmol/L). (K) MST analysis of BD binding to the mutant ICAT (K_d = 250 μmol/L). Data are shown as mean ± SD (n = 3). *P < 0.05, **P < 0.01, and ***P < 0.001 *versus* the control group.

ICAT tended to significantly decrease with a K_d estimated at 250 μmol/L (Fig. 5K). This result further confirmed the important role of Lys28 in BD binding with ICAT.

3.5. *Effect of silencing ICAT on the glucose metabolism in HCC cells under hypoxic conditions*

To further validate the effects of BD on β-catenin and HIF-1α signaling through ICAT, we first knocked down ICAT using a ICAT siRNA (si-ICAT) on HepG2 and Huh7 cells (Supporting Information Fig. S3). ICAT knockdown significantly reversed the inhibition effect of BD on the HIF-1α and its downstream glycolytic pathway, including LDHA, GLUT1/3, HK2, and PKM2 (Fig. 6A−D). In addition, ICAT knockdown alleviated the inhibition effect of BD on glucose uptake and L-lactate production in HCC cells (Fig. 6E−G). These results indicate an important role of ICAT in BD induced β-catenin/HIF-1α inhibition and downstream glycolysis.

3.6. *BD disrupted the interaction between ICAT and β-catenin*

ICAT was firstly demonstrated as a β-catenin interacting protein that blocked the interaction between β-catenin and TCF/LEF[25]. Interestingly, a recent report indicated that ICAT also could stabilize β-catenin through competing with adenomatous polyposis coli (APC) for binding to β-catenin, diminishing the function of β-catenin destruction complex[26].

As shown in Fig. 6H and I, BD could inhibit the expression of β-catenin under hypoxia in a dose-dependent manner, while β-catenin was increased in co-existence of BD and MG-132 compared with that in the presence of BD alone (Supporting Information Fig. S4). This difference suggested that BD-induced inhibition of β-catenin occurs *via* the proteasome-dependent pathway, which was consistent with our previous report[15]. These findings raised the interesting possibility that BD could promote β-catenin degradation through blocking the interaction between ICAT and β-catenin. To verify this hypothesis, we performed a co-immunoprecipitation (Co-IP) assay to investigate whether BD

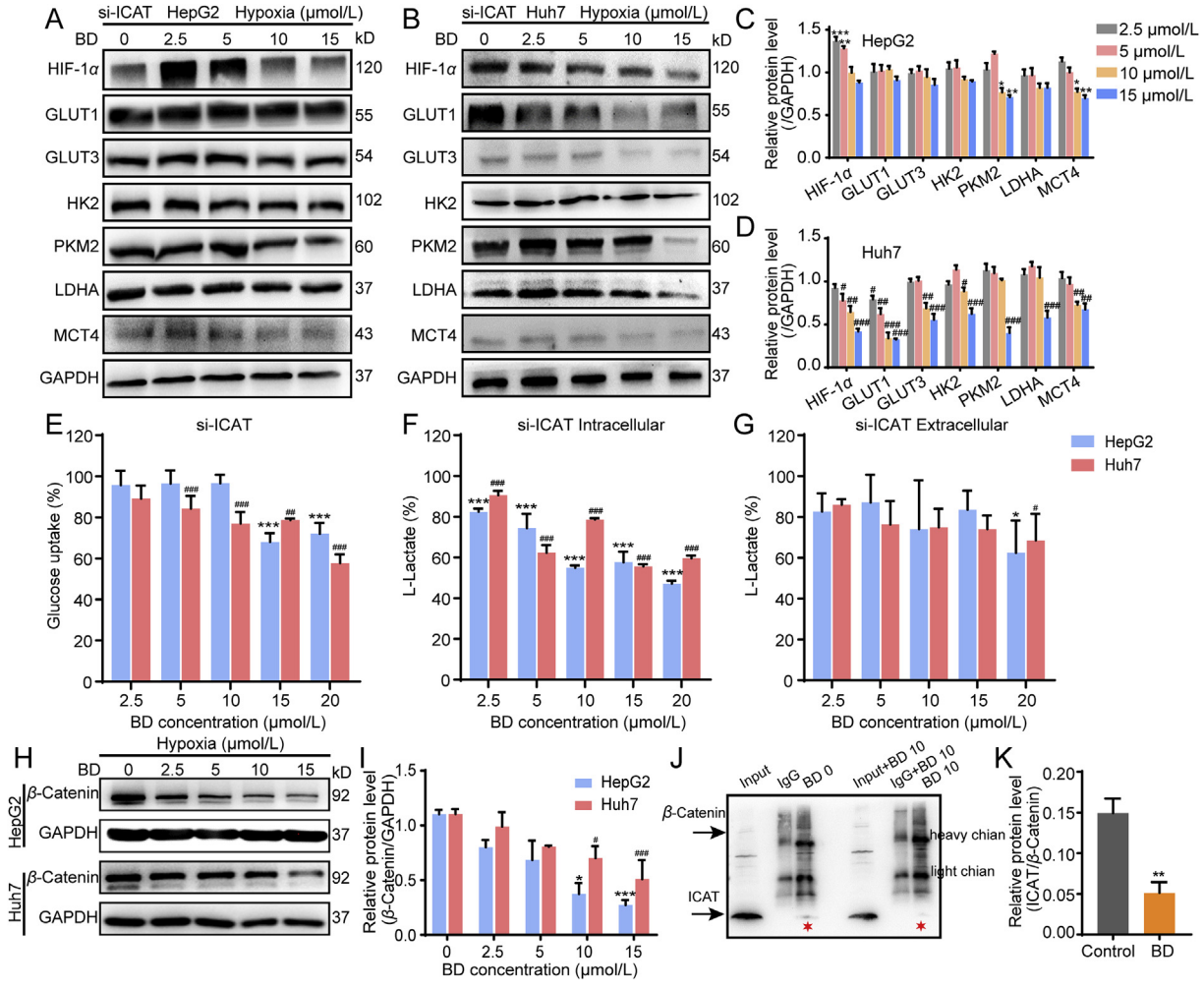

Figure 6 Knockdown of ICAT increased the resistance to BD treatment, BD disrupted the interaction of ICAT and β-catenin. Repression of ICAT by siRNA significantly reversed the inhibition effect of BD on the HIF-1α and its mediated glucose metabolic pathway in HepG2 (A and C) and Huh7 cells (B and D). Relative glucose uptake in si-ICAT HCC cells treated with BD for 24 h (E). Relative lactate production in si-ICAT HCC cells with BD for 24 h (F and G). BD inhibited the expression of β-catenin under hypoxia in HCC cells (H and I). Co-IP assay revealed that BD disturb the interaction between β-catenin and ICAT (J and K). Data are shown as mean ± SD ($n = 3$). * and $^{\#}P < 0.05$, ** and $^{\#\#}P < 0.01$, *** and $^{\#\#\#}P < 0.001$ *versus* the control group.

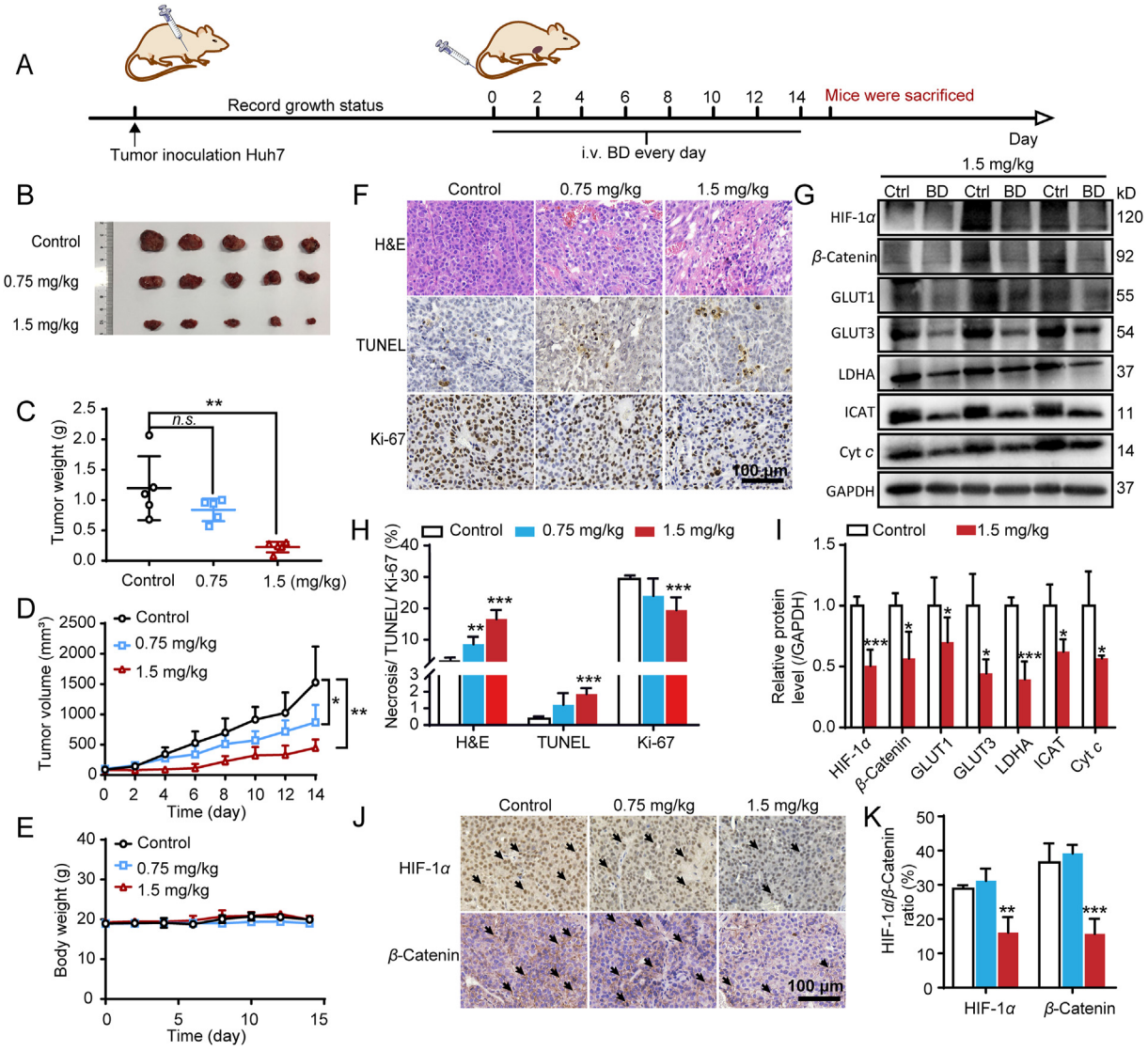

Figure 7 BD suppressed tumor growth and the protein expression of HIF-1α and its metabolism-related target genes in the Huh7 xenograft model. (A) Schematic plan for the administration of BD (0.75 and 1.5 mg/kg/day). The tumor weight (C), tumor volume (D), and the mice body weight (E) were monitored every two days till Day 14, when mice were sacrificed and the resected tumors were photographed (B) and processed for pathological and immunohistochemical assay for the necrosis area, TUNEL, Ki-67, HIF-1α, and β-catenin positive tumor cells (F, H, and J, K). Western blotting assay shows that BD treatment inhibited HIF-1α and its metabolism-related target genes *in vivo* (G and I). Scale bars = 100 μm. Data are shown as mean ± SD (n = 3). *$P < 0.05$, **$P < 0.01$, ***$P < 0.001$ *versus* the control group.

could inhibit the protein-protein interaction between β-catenin and ICAT. This result revealed that BD attenuated the direct binding between β-catenin and ICAT in ICAT-overexpressing HepG2 cells, while the expression of total ICAT did not change (Fig. 6J and K). And the expression of HIF-1α was significantly decreased after β-catenin knockdown (Supporting Information Fig. S5), which was consistent with previous study[14]. Several studies indicated that β-catenin might indirectly affect the expression of HIF-1α though the WNT responsive gene *c-MYC*[27–29].

Then the mechanism of BD inhibits the expression of HIF-1α was further investigated. As shown in Supporting Information Fig. S6A, HIF-1α rapidly accumulated in the presence of proteasome inhibitor MG-132 under hypoxia. In contrast, BD inhibited HIF-1α accumulation even co-treatment with MG-132, indicating that BD impaired the protein synthesis of HIF-1α. By co-treating with protein translation inhibitor cycloheximide (CHX) reflected that BD did not modify the degradation rate of HIF-1α (Figs. S6C and S6D). And the results of qRT-PCR show that there was no reduction in the mRNA level of HIF-1α after treating with BD under hypoxia (Fig. S6B), indicating that BD suppressed the translation of HIF-1α to inhibit its synthesis.

These results suggest that BD directly targeted ICAT to disturb the interaction between ICAT and β-catenin, and promoted the degradation of β-catenin which was involved with HIF-1α expression.

3.7. *BD suppressed the growth of xenograft tumors*

Finally, to evaluate the anti-tumor activity of BD *in vivo*, we performed BD treatment assay on the Huh7 xenograft model, and the experimental mice were treated with BD at dosage of 0.75 and 1.5 mg/kg/day *via* tail vain injection for consecutive two weeks (Fig. 7A). The group treated with BD of 1.5 mg/kg/day significantly inhibited Huh7 tumor growth compared with control ones

without significant body weight loss or side effects in all the treated mice (Fig. 7B−E).

Pathological and immunohistochemical analysis of tumor sections shows that BD (1.5 mg/kg/day) led to significantly increased necrosis area, TUNEL-positive cells and decreased Ki67 positive cells compared with control group (Fig. 7F−H). Consistent with the findings *in vitro*, BD could decrease the protein levels of HIF-1α, β-catenin, GLUT1/3, LDHA, ICAT and Cyt *c* in tumors (Fig. 7G and 7I−K).

4. Discussion

According to data from World Health Organization (WHO), HCC is currently the fourth most common cause of cancer-related deaths[30]. While the incidence and mortality for other cancers is declining, HCC still represents an increasingly significant public health problem[1]. Despite encouraging advances in its treatment, most patients die in one year after diagnosis largely because of the easy recurrence and metastases[31]. And since the successful approval of sorafenib (2008), several clinical trials have attempted to evaluate different options for the treatment of HCC, however, few to be effective[3].

As the results of excessive metabolic activity and non-functioning vascularization, hypoxia has become a prominent feature of tumor, associating with poor prognosis and drug resistance[32]. HIF-1α has been proved to mediate expression of genes involved in every step of HCC metastasis including EMT, intravasation and extravasation, and the secondary growth of metastases[4]. HIF-1α expression in HCC has been regarded as a poor prognostic indicator in clinic and is associated with metastatic potential[14]. In addition, the antiangiogenic effects of sustained sorafenib treatment promotes intratumoral hypoxia and HIF-1α-mediated cellular responses that favor the selection of resistant cancer cells[32,33]. Thus, the combination of current sorafenib treatment with gene therapy or inhibitors against HIFs have been documented as promising approaches to overcome resistance[32,33]. In our previous study, we identified a natural product, BD, which suppressed HCC growth by inducing β-catenin degradation[15]. Notably, BD also potentiated sorafenib therapeutic effects in an HCC orthotopic model[15]. Recently, several studies have focused on the crosstalk between β-catenin and HIF-1α. β-Catenin, through enhancing HIF-1 transcriptional activity, can promote HCC and colon cancer-cell survival under hypoxic conditions[14,34,35].

In this research, we identified BD could significantly inhibit the expression of HIF-1α and subsequent mediated HCC cell metabolism, including mitochondrial oxidative phosphorylation, aerobic glycolysis, ROS accumulation, intercellular and extracellular L-lactate concentrations, as well as ATP levels. Using biophysical proteomics approaches, we identified β-catenin-interacting protein 1 (ICAT) as the functional target of BD. The MST and docking results indicated that BD could bind to ICAT through hydrogen bonds of Lys28, and hydrophobic interaction of Leu24, Leu52, and Met25. It is important to note that the other potential sites in the binding pocket, including Gln54, Gln51, and Arg27, cannot be used to form hydrogen bond either by far spatial distance (>4 Å) or no corresponding functional groups on BD. This may explain the reason for only one hydrogen bond formed in the reported docking assay. In addition, Ji et al.[26] proved that ICAT could block the APC-β-catenin interaction, inhibit the β-catenin destruction complex, and stabilize β-catenin. Here, we demonstrated that BD could disrupt the direct interaction between ICAT and β-catenin, inducing β-catenin degradation, which in turn induced the decrease of HIF-1α expression. Furthermore, BD could inhibit HCC cells proliferation and tumor growth *in vivo*, and knockdown of ICAT substantially increased resistance to BD treatment *in vitro*. It is worth noting that, BD still exhibited inhibition effects at high concentration (10 and 15 μmol/L) after silencing ICAT. According to these results and previous reports[8,12,36,37], we speculate that BD may also have other molecular targets despite the key role of ICAT in hypoxic HCC cells. Overall, our data highlight the potential of BD as a modulator of β-catenin/HIF-1α axis mediated HCC metabolism.

5. Conclusions

An isolated natural product, BD, was identified as selectively binding with ICAT which inhibited HIF-1α expression. BD suppressed hepatocellular carcinoma cell growth both *in vitro* and in xenograft models by inhibiting HIF-1α mediated cell metabolism. Results from this study provide insights into the development of novel HIF-1α inhibitor, with BD being a potential leading compound for further development.

Acknowledgments

This work was supported by the National Natural Science Foundation of China (No.81903654 and 81773941), Program for Professor of Special Appointment (Young Eastern Scholar) at Shanghai Institutions of Higher Learning (QD2018035, China), Shanghai "Chenguang Program" of Education Commission of Shanghai Municipality (No.18CG46, China), Shanghai Sailing Program (No.19YF1449400, China), Ruijin Youth NSFC Cultivation Fund (KY20194297, China), National Key Subject of Drug Innovation (2019ZX09201005-007, China), National Key R&D Program for key research project of modernization of traditional Chinese medicine (2019YFC1711602, China).

Author contributions

Weidong Zhang, Xin Luan, Hongzhuan Chen: conceptualization, original draft, methodology, review and editing, funding acquisition and supervision. Rui Huang, Lijun Zhang, Jinmei Jin: carried out the experiment, made figures and wrote the paper. Hongwei Zhang, Dong Lu, Yudong Zhou, Hong Zhang, Chao Lv, Ye Wu, and Sanhong Liu analyzed the data and revised the paper.

Conflicts of interests

The authors have declared that no competing interest exists.

Appendix A. Supporting information

Supporting data to this article can be found online at https://doi.org/10.1016/j.apsb.2021.05.009.

References

1. Siegel RL, Miller KD, Jemal A. Cancer statistics. *CA Cancer J Clin* 2020;**70**:7−30.
2. Zhang X, Zhang P, An L, Sun N, Peng L, Tang W, et al. Miltirone induces cell death in hepatocellular carcinoma cell through GSDME-dependent pyroptosis. *Acta Pharm Sin B* 2020;**10**:1397−413.

3. Yang JD, Hainaut P, Gores GJ, Amadou A, Plymoth A, Roberts LR. A global view of hepatocellular carcinoma: trends, risk, prevention and management. *Nat Rev Gastroenterol Hepatol* 2019;**16**:589−604.
4. Wilson GK, Tennant DA, McKeating JA. Hypoxia inducible factors in liver disease and hepatocellular carcinoma: current understanding and future directions. *J Hepatol* 2014;**61**:1397−406.
5. Zhao C, Zeng C, Ye S, Dai X, He Q, Yang B, et al. Yes-associated protein (YAP) and transcriptional coactivator with a PDZ-binding motif (TAZ): a nexus between hypoxia and cancer. *Acta Pharm Sin B* 2020;**10**:947−60.
6. Lin D, Wu J. Hypoxia inducible factor in hepatocellular carcinoma: a therapeutic target. *World J Gastroenterol* 2015;**21**:12171−8.
7. Wong CC, Kai AK, Ng IO. The impact of hypoxia in hepatocellular carcinoma metastasis. *Front Med* 2014;**8**:33−41.
8. Fan J, Ren D, Wang J, Liu X, Zhang H, Wu M, et al. Bruceine D induces lung cancer cell apoptosis and autophagy *via* the ROS/MAPK signaling pathway *in vitro* and *in vivo*. *Cell Death Dis* 2020;**11**:126.
9. Xu W, Jiang X, Xu Z, Ye T, Shi Q. The efficacy of brucea javanica oil emulsion injection as adjunctive therapy for advanced non-small-cell lung cancer: a meta-analysis. *Evid Based Complement Alternat Med* 2016;**2016**:5928562.
10. Luo D, Hou D, Wen T, Feng M, Zhang H. Efficacy and safety of *Brucea javanica* oil emulsion for liver cancer: a protocol for systematic review and meta-analysis. *Medicine* 2020;**99**:e23197.
11. Wu JR, Liu SY, Zhu JL, Zhang D, Wang KH. Efficacy of *Brucea iavanica* oil emulsion injection combined with the chemotherapy for treating gastriccancer: a systematic review and meta-analysis. *Evid Based Complement Alternat Med* 2018;**2018**:6350782.
12. Lau ST, Lin ZX, Liao Y, Zhao M, Cheng CH, Leung PS. Bruceine D induces apoptosis in pancreatic adenocarcinoma cell line PANC-1 through the activation of p38-mitogen activated protein kinase. *Cancer Lett* 2009;**281**:42−52.
13. Zhang JY, Lin MT, Tung HY, Tang SL, Yi T, Zhang YZ, et al. Bruceine D induces apoptosis in human chronic myeloid leukemia K562 cells *via* mitochondrial pathway. *Am J Cancer Res* 2016;**6**:819−26.
14. Liu L, Zhu XD, Wang WQ, Shen Y, Qin Y, Ren ZG, et al. Activation of β-catenin by hypoxia in hepatocellular carcinoma contributes to enhanced metastatic potential and poor prognosis. *Clin Cancer Res* 2010;**16**:2740−50.
15. Cheng Z, Yuan X, Qu Y, Li X, Wu G, Li C, et al. Bruceine D inhibits hepatocellular carcinoma growth by targeting β-catenin/Jagged1 pathways. *Cancer Lett* 2017;**403**:195−205.
16. Xie JX, Ji Z. The chemical constituents of the Chinese drug "Yadanzi". I. Isolation and identification of daucosterol, brucein D and brucein E (author's transl.). *Acta Pharm Sin* 1981;**16**:53−5.
17. Khavrutskii L, Yeh J, Timofeeva O, Tarasov SG, Pritt S, Stefanisko K, et al. Protein purification-free method of binding affinity determination by microscale thermophoresis. *J Vis Exp* 2013;**78**:50541.
18. Qu Y, Olsen JR, Yuan X, Cheng PF, Levesque MP, Brokstad KA, et al. Small molecule promotes β-catenin citrullination and inhibits Wnt signaling in cancer. *Nat Chem Biol* 2018;**14**:94−101.
19. Semenza GL. HIF-1 mediates metabolic responses to intratumoral hypoxia and oncogenic mutations. *J Clin Invest* 2013;**123**:3664−71.
20. Guo Y, Liang F, Zhao F, Zhao J. Resibufogenin suppresses tumor growth and Warburg effect through regulating miR-143-3p/HK2 axis in breast cancer. *Mol Cell Biochem* 2020;**466**:103−15.
21. Zhang BB, Wang DG, Guo FF, Xuan C. Mitochondrial membrane potential and reactive oxygen species in cancer stem cells. *Fam Cancer* 2015;**14**:19−23.
22. Zorova LD, Popkov VA, Plotnikov EY, Silachev DN, Pevzner IB, Jankauskas SS, et al. Mitochondrial membrane potential. *Anal Biochem* 2018;**552**:50−9.
23. Ow YP, Green DR, Hao Z, Mak TW. Cytochrome *c*: functions beyond respiration. *Nat Rev Mol Cell Bio* 2008;**9**:532−42.
24. Daniels DL, Weis WI. ICAT inhibits β-catenin binding to Tcf/Lef-family transcription factors and the general coactivator p300 using independent structural modules. *Mol Cell* 2002;**10**:573−84.
25. Sekiya T, Nakamura T, Kazuki Y, Oshimura M, Kohu K, Tago K, et al. Overexpression of *Icat* induces G_2 arrest and cell death in tumor cell mutants for *Adenomatous polyposis coli*, *β-catenin*, or *Axin*. *Cancer Res* 2002;**62**:3322−6.
26. Ji L, Lu B, Wang Z, Yang Z, Reece-Hoyes J, Russ C, et al. Identification of ICAT as an APC inhibitor, revealing Wnt-dependent inhibition of APC−Axin interaction. *Mol Cell* 2018;**72**:37−47.
27. Zhang J, Sattler M, Tonon G, Grabher C, Lababidi S, Zimmerhackl A, et al. Targeting angiogenesis *via* a c-Myc/hypoxia-inducible factor-1alpha-dependent pathway in multiple myeloma. *Cancer Res* 2009;**69**:5082−90.
28. Liu X, Zhou Y, Peng J, Xie B, Shou Q, Wang J. Silencing c-Myc enhances the antitumor activity of bufalin by suppressing the HIF-1α/SDF-1/CXCR4 pathway in pancreatic cancer cells. *Front Pharmacol* 2020;**11**:495.
29. Vallee A, Guillevin R, Vallee JN. Vasculogenesis and angiogenesis initiation under normoxic conditions through Wnt/β-catenin pathway in gliomas. *Rev Neurosci* 2018;**29**:71−91.
30. Villanueva A. Hepatocellular carcinoma. *N Engl J Med* 2019;**380**:1450−62.
31. Ogunwobi OO, Harricharran T, Huaman J, Galuza A, Odumuwagun O, Tan Y, et al. Mechanisms of hepatocellular carcinoma progression. *World J Gastroenterol* 2019;**25**:2279−93.
32. Mendez-Blanco C, Fondevila F, Garcia-Palomo A, Gonzalez-Gallego J, Mauriz JL. Sorafenib resistance in hepatocarcinoma: role of hypoxia-inducible factors. *Exp Mol Med* 2018;**50**:1−9.
33. Liang Y, Zheng T, Song R, Wang J, Yin D, Wang L, et al. Hypoxia-mediated sorafenib resistance can be overcome by EF24 through Von Hippel-Lindau tumor suppressor-dependent HIF-1α inhibition in hepatocellular carcinoma. *Hepatology* 2013;**57**:1847−57.
34. Kaidi A, Williams AC, Paraskeva C. Interaction between β-catenin and HIF-1 promotes cellular adaptation to hypoxia. *Nat Cell Biol* 2007;**9**:210−7.
35. Zhang Q, Bai X, Chen W, Ma T, Hu Q, Liang C, et al. Wnt/β-catenin signaling enhances hypoxia-induced epithelial-mesenchymal transition in hepatocellular carcinoma *via* crosstalk with Hif-1α signaling. *Carcinogenesis* 2013;**34**:962−73.
36. Tan B, Huang Y, Lan L, Zhang B, Ye L, Yan W, et al. Bruceine D induces apoptosis in human non-small cell lung cancer cells through regulating JNK pathway. *Biomed Pharmacother* 2019;**117**:109089.
37. Wang S, Hu H, Zhong B, Shi D, Qing X, Cheng C, et al. Bruceine D inhibits tumor growth and stem cell-like traits of osteosarcoma through inhibition of STAT3 signaling pathway. *Cancer Med* 2019;**8**:7345−58.